

Characterization of forced degradation products of ketorolac tromethamine using LC/ESI/Q/TOF/MS/MS and *in silico* toxicity prediction

Pradipbhai D. Kalariya,^a B. Raju,^b Roshan M. Borkar,^b Deepak Namdev,^a S. Gananadhamu,^a Prajwal P. Nandekar,^c Abhay T. Sangamwar^c and R. Srinivas^{a,b*}

Ketorolac, a nonsteroidal anti-inflammatory drug, was subjected to forced degradation studies as per International Conference on Harmonization guidelines. A simple, rapid, precise, and accurate high-performance liquid chromatography combined with electrospray ionization quadrupole time-of-flight tandem mass spectrometry (LC/ESI/Q/TOF/MS/MS) method has been developed for the identification and structural characterization of stressed degradation products of ketorolac. The drug was found to degrade in hydrolytic (acidic, basic, and neutral), photolytic (acidic, basic, and neutral solution), and thermal conditions, whereas the solid form of the drug was found to be stable under photolytic conditions. The method has shown adequate separation of ketorolac tromethamine and its degradation products on a Grace Smart C-18 (250 mm × 4.6 mm i.d., 5 μm) column using 20 mM ammonium formate (pH = 3.2): acetonitrile as a mobile phase in gradient elution mode at a flow rate of 1.0 ml/min. A total of nine degradation products were identified and characterized by LC/ESI/MS/MS. The most probable mechanisms for the formation of degradation products have been proposed on the basis of a comparison of the fragmentation of the [M + H]⁺ ions of ketorolac and its degradation products. *In silico* toxicity of the drug and degradation products was investigated by using TOPKAT and DEREK softwares. The method was validated in terms of specificity, linearity, accuracy, precision, and robustness as per International Conference on Harmonization guidelines. Copyright © 2014 John Wiley & Sons, Ltd.

Keywords: ketorolac tromethamine; anti-inflammatory; forced degradation; LC/ESI/MS/MS; accurate mass measurements; degradation products; *in silico* toxicity

Introduction

Ketorolac tromethamine (KETO) [(±) 5-benzoyl-2,3 dihydro-1H-pyrrolizine-1-carboxylic acid, 2-amino-2-(hydroxymethyl)-1,3-propanediol] is a nonsteroidal anti-inflammatory drug with an analgesic efficacy, 800 times more potent than aspirin. It has both anti-inflammatory and analgesic activity.^[1] KETO is mainly used in the treatment of postsurgical ocular pain and allergic conjunctivitis.^[2] It is associated with a high risk of serious gastrointestinal toxicity, peptic ulceration, and acute renal failure.^[3] Concerns about the severe side effects of KETO led to restriction in its dosage and maximum duration of use for tablets and intravenous or intramuscular formulation.

Stress stability is an integral part of the drug development process and explains several factors that affect the expiration dating of drug products, including the chemical and physical stability during the preclinical formulation stages, process development, packaging development, and postmarketing life. As per the regulatory guidelines,^[4,5] it is essential to establish the stability indicating assay method that gives the idea of inherent stability of the drug. Characterization of degradants is useful to establish the mechanism of formation of degradation product (DP) of the drug and the explanation of side effects of drugs.^[6] Recently, we have reported the structural characterization of DPs of drugs

formed under various stress conditions by LC/MS/MS in combination with accurate mass measurements.^[7–10]

A few analytical and bioanalytical methods have been reported in the literature for the determination of KETO alone or in combination with other drugs. It includes determination of KETO in biological samples by using LC and LC/MS methods^[11–21] as well as LC/MS/MS method,^[22] *in vivo* metabolites identification,^[23] spectrophotometric estimation of KETO by different methods,^[24] determination of KETO by HPTLC,^[25] determination of KETO and its impurities by capillary electrochromatography,^[26] assay of KETO in pharmaceutical matrices using differential pulse polarography,^[27] derivative adsorptive

* Correspondence to: R. Srinivas, National Centre for Mass Spectrometry, CSIR-Indian Institute of Chemical Technology, Hyderabad, 500 007, AP, India. E-mail: srini@iict.res.in; sragampeta@yahoo.co.in

a Department of Pharmaceutical Analysis, National Institute of Pharmaceutical Education and Research (NIPER), Balanagar, Hyderabad, 500037, AP, India

b National Centre for Mass Spectrometry, CSIR-Indian Institute of Chemical Technology, Hyderabad, 500 007, AP, India

c Department of Pharmacoinformatics, National Institute of Pharmaceutical Education and Research (NIPER), Sector 67, S.A.S. Nagar (Mohali), Punjab, 160 062, India

chronopotentiometry,^[28] and high-performance liquid chromatography (HPLC) methods.^[29–31]

The hydrolytic degradation behavior of KETO was studied under acidic and alkaline conditions by Salaris *et al.*^[32] One acid hydrolysis product was identified that is listed in British Pharmacopoeia as impurity H, chemically known as methyl (1RS)-5-benzoyl-2,3-dihydro-1H-pyrrolizine-1-carboxylate (Scheme 1, structure **K-8**). A drug substance monograph of KETO in British Pharmacopoeia'09 listed ten impurities.^[33] However, the listed impurities are not classified into DPs and process impurities.

There is no systematic study on the degradation behavior of ketorolac including developing a stability indicating method, validation of the method, and characterization of all the DPs formed under ICH recommended stress conditions using LC/ESI/MS/MS. Even the roles of other stress conditions (e.g. oxidation, photolysis, and thermal) on the chemical stability of KETO are important. Hence, the purpose of the present study was to develop a stability indicating method for KETO and to characterize using LC/ESI/MS/MS all the DPs formed under the International Conference on Harmonization (ICH) recommended stress conditions. The results of the present study may also be helpful for the assessment of the quality of store products that have expired or on the edge of getting expired. By considering this information additionally, *in silico* toxicity and carcinogenicity of all the proposed degradants was predicted using TOPKAT (toxicity prediction by computer-assisted technology) and DEREK (deductive estimate of risk from existing knowledge) softwares. Some of the DPs may possess potential for genotoxicity, which create an additional safety concern leading to significant risk for carcinogenicity or other toxic effects.

Experimental

Materials and reagents

Pure ketorolac was obtained as a gift from Symed Labs Hyderabad, India. HPLC grade acetonitrile was purchased from S. D. Fine Chemicals (Mumbai, India). All analytical grade reagents: ammonium formate, formic acid, sodium hydroxide, hydrochloric acid, and 6%

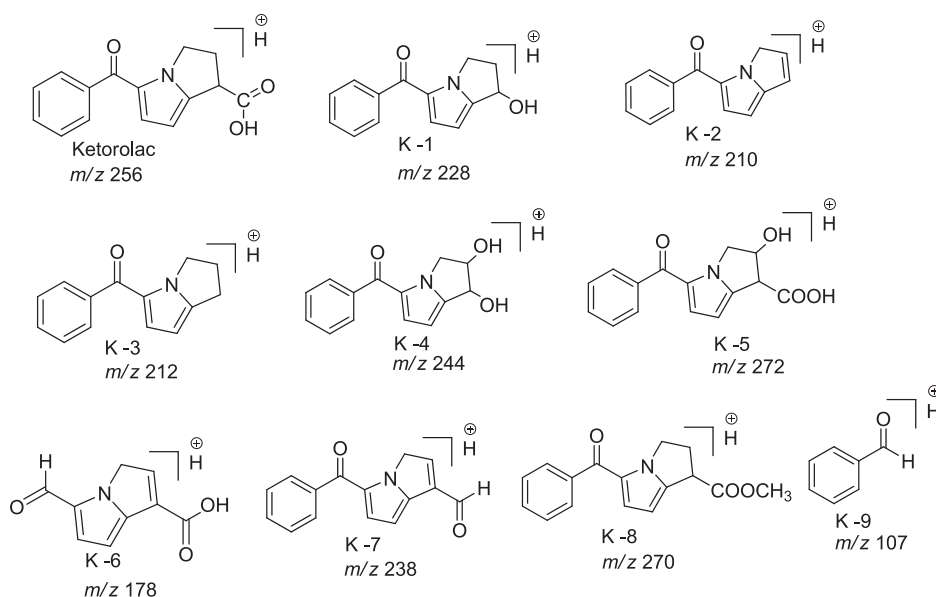
(w/w) hydrogen peroxide were purchased from Merck (Mumbai, India). HPLC grade water was prepared by filtering through a Millipore Milli-Q- plus system (Millipore, Milford, MA, USA).

Instrumentation and software

The HPLC analysis was performed on Shimadzu separation module consisting of a binary pump (LC-20 AD); photodiode array detector (SPD-M20A) and degasser (DGU-20A3). The output signal was monitored and processed using LC-Solution software. All pH measurements were carried out on a glass electrode containing pH meter, pH tutor (Eutech Instruments), and weighing was carried out on a Sartorius balance (CPA225D, Germany).

For LC/MS analysis, an Agilent 1200 series HPLC instrument (Agilent Technologies, USA) attached to a quadrupole time-of-flight (Q-TOF) mass spectrometer (Q-TOF LC/MS 6510 series classic G6510A, Agilent Technologies, USA) equipped with an electrospray ionization (ESI) source. The data acquisition was under the control of Mass Hunter workstation software. The typical operating source conditions for MS scan of KETO in positive ESI mode were optimized as follows: the fragmentor voltage was set at 70 V, the capillary at 3500 V, the skimmer at 60 V, and nitrogen was used as the drying (320 °C, 10 l/min) and nebulizing (45 psi) gas. For collision-induced dissociation experiments, keeping MS1 static, the precursor ion of interest was selected using the quadrupole analyzer, and the product ions were analyzed using the TOF analyzer. Ultrahigh pure nitrogen gas was used as collision gas. All the spectra were recorded under identical experimental conditions and were an average of 20–25 scans.

Photolytic studies were carried out in a photostability chamber (Osworld OPSH-G-16-GMP series, Osworld Scientific Equipments Pvt. Ltd. India) set at 40.0 ± 5.0 °C/75.0% relative humidity (RH) ± 3.0% RH and equipped with an illumination bank on inside top, consisting of a combination of two black light ultraviolet lamps and four white fluorescent lamps in accordance with two option of the ICH guideline Q1B. Assessment of *in silico* toxicity was carried out by using TOPKAT (Discovery Studio 2.5, Accelrys, Inc., San Diego, CA, USA) and DEREK (Nexus v 2.0, Lhasa Ltd., Leeds, UK) software.



Scheme 1. Proposed structures of protonated degradation products of ketorolac tromethamine formed under various stress conditions.

Forced degradation studies

Forced degradation of KETO was carried out on the bulk drug (KETO) as per ICH guidelines Q1A (R2). KETO was subjected to stress hydrolytic degradation study by refluxing 24 h in acidic (1.0 N HCl), 24 h in alkaline (1.0 N NaOH), and 72 h in neutral (H₂O) conditions. The optimized oxidative, photolytic, and thermal stress conditions are given in Table 1. The drug solutions were prepared in 1.0 mg/ml concentration for all stress samples.

Sample preparation

All the stressed samples (hydrolytic, oxidative, thermal, and photolytic stress) were neutralized and diluted with mobile phase and filtered through 0.22 µm membrane filter before LC/MS analysis.

Results and discussion

Chromatographic conditions

Chromatographic conditions were optimized using a Grace smart C₁₈ column (250 mm × 4.6 mm, 5 µm) with a mobile phase composed of ammonium formate buffer (A) (pH 3.2; 20 mM, pH adjusted by formic acid) and acetonitrile (B) in a gradient mode. A linear flow gradient program was set as follows: 0/20, 5/20, 7/30, 9/45, 18/55, 22/45, and 28/20 (T_{min}/%B) where all the DPs of KETO eluted at adequate retention times (Rt) with good resolution and symmetrical peak shapes. The column temperature, flow rate, injection volume, and detector wavelength were at 30 °C, 1.0 ml/min, 20.0 µl, and 280 nm, respectively. For LC/MS analysis, conditions such as nebulizing gas flow, drying gas temperature, capillary voltage, drying gas flow, skimmer voltage, and spray voltage were optimized once more to obtain maximum ionization of KETO and all the DPs. The method was validated with respect to the parameters given in ICH guidelines Q1A (R2).^[34]

Degradation behavior of KETO

The degradation behavior of KETO was studied using LC/MS under various forced degradation conditions. Sufficient degradation was observed in all conditions except in solid photolysis where drug was found to be stable. The overlay of LC/ESI/MS total ion chromatograms of all stress degradation samples are given in

Fig. 1. A total of nine DPs were identified and characterized by using LC/ESI/MS/MS experiments and accurate mass measurements. The proposed structures of DPs and their elemental compositions are given in Scheme 1 and Table 2.

Hydrolysis

Initially, KETO was refluxed in 0.5 N HCl and 0.5 N NaOH at 80 °C for 24 h. Drug was found to be stable in these conditions. While three DPs (**K-1** to **K-3**) were formed in 1.0 N HCl at 80 °C for 24 h (Fig. 1(A)), only one DP (**K-3**) was formed in 1.0 N NaOH at 80 °C for 24 h (Fig. 1(B)). In neutral hydrolysis, one DP, **K-3**, was

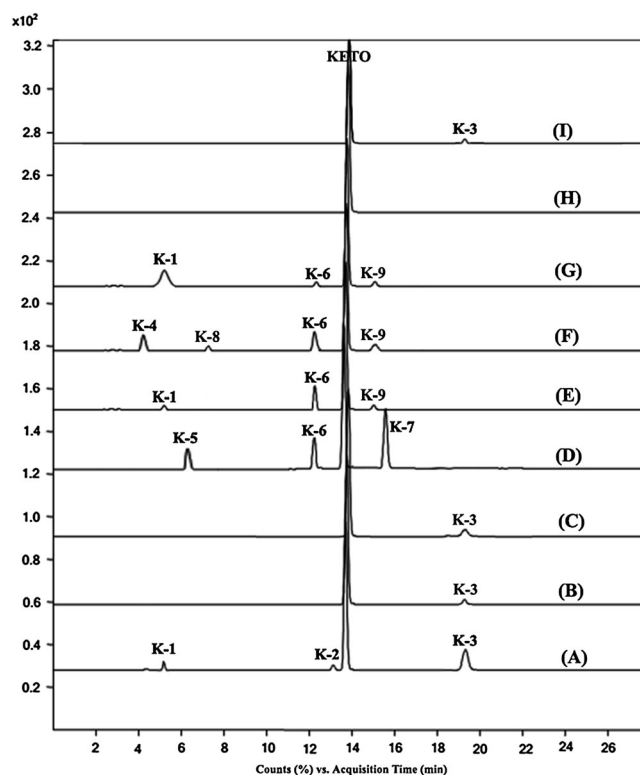


Figure 1. LC/ESI/MS/TIC of (A) acidic, (B) basic, (C) neutral, (D) oxidative, (E) photo neutral, (F) photo acidic, (G) photo basic, (H) photo solid, and (I) thermal degradation products.

Table 1. Stress conditions for optimum degradation of ketorolac tromethamine (KETO)				
Stress conditions	Concentration of stressors	Exposure condition (°C)	Duration	Percent degradation of KETO
Hydrolysis				
Acid	1.0 N HCl	80	24 h	18.5
Base	1.0 N NaOH	80	24 h	6.2
Neutral	H ₂ O	80	72 h	5.5
Oxidation	6.0% H ₂ O ₂	Room temperature	15 days	30.5
Photolysis				
Acid	0.1 N HCl	40, 75% RH	15 days	15.2
Base	0.1 N NaOH	40, 75% RH		14.8
Neutral	H ₂ O	40, 75% RH		11.9
Solid	—	40, 75% RH		0.0
Thermal	—	70	15 days	5.8

RH, relative humidity.

Table 2. Elemental composition of ketorolac tromethamine (KETO) and degradation products

Degradation product	Retention time (min)	Molecular formula [M+H] ⁺	Calculated m/z	Observed m/z	Error (ppm)	MS/MS fragment ions
KETO	13.8	C ₁₅ H ₁₄ NO ₃ ⁺	256.0968	256.0962	2.64	210, 178, 132, 105, 77
K-1	5.1	C ₁₄ H ₁₄ NO ₂ ⁺	228.1018	228.1014	1.75	200, 184, 150, 105, 77
K-2	13.1	C ₁₄ H ₁₂ NO ⁺	210.0914	210.0911	1.43	192, 132, 105, 77
K-3	19.3	C ₁₄ H ₁₄ NO ⁺	212.1080	212.1082	-0.94	194, 184, 134, 105
K-4	4.1	C ₁₄ H ₁₄ NO ₃ ⁺	244.0967	244.0961	2.46	226, 216, 198, 170, 158
K-5	6.2	C ₁₅ H ₁₄ NO ₄ ⁺	272.0913	272.0911	0.74	254, 194, 105
K-6	12.3	C ₉ H ₈ NO ₃ ⁺	178.0490	178.0488	1.12	—
K-7	15.5	C ₁₅ H ₁₂ NO ₂ ⁺	238.0863	238.0861	0.84	—
K-8	7.2	C ₁₆ H ₁₆ NO ₃ ⁺	270.1135	270.1131	1.48	210, 105
K-9	15.0	C ₇ H ₇ O ⁺	107.0496	107.0495	0.93	77

observed by refluxing the drug in water at 80 °C for 3 days (Fig. 1 (C)) (Schemes 2–4).

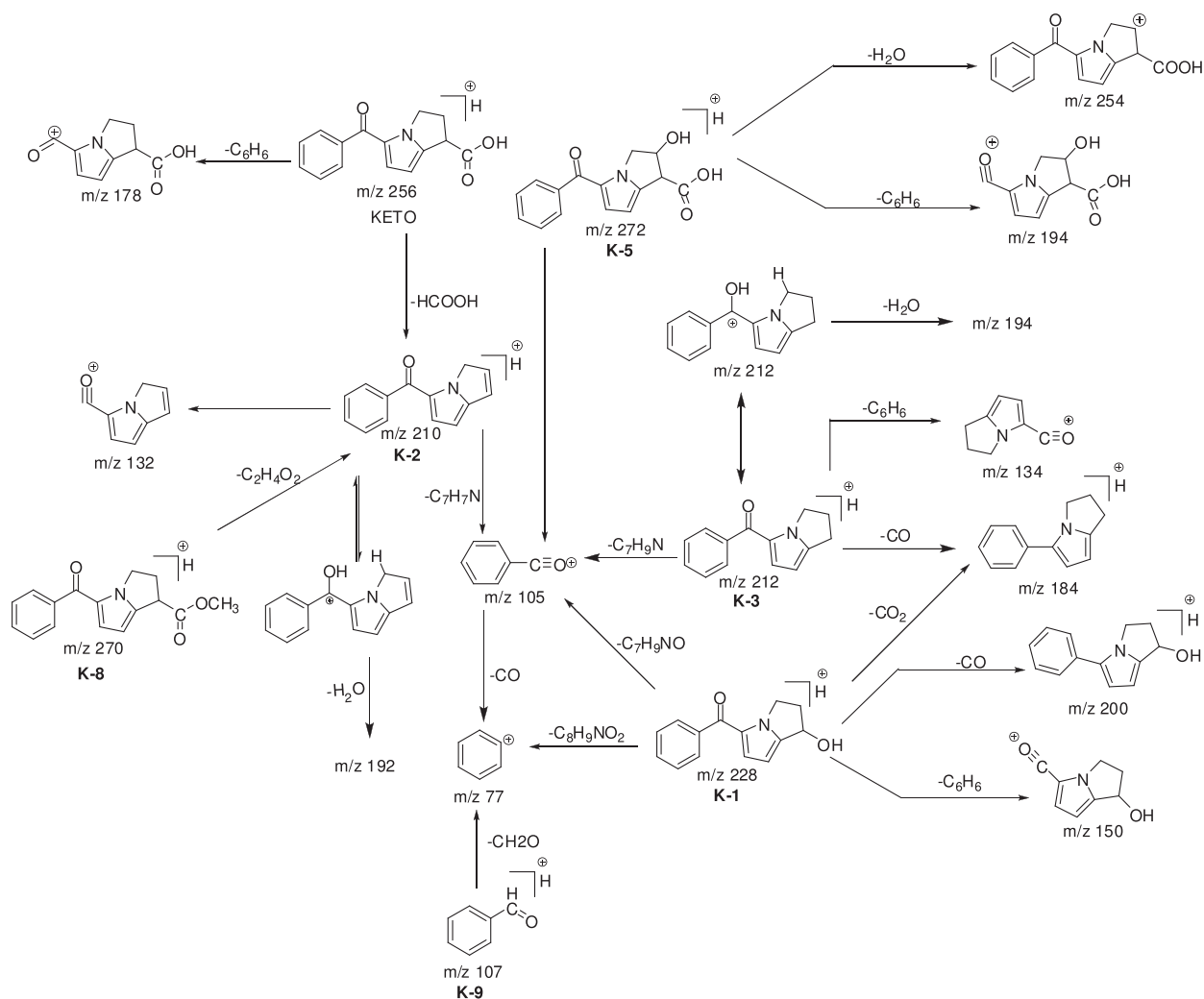
Oxidation

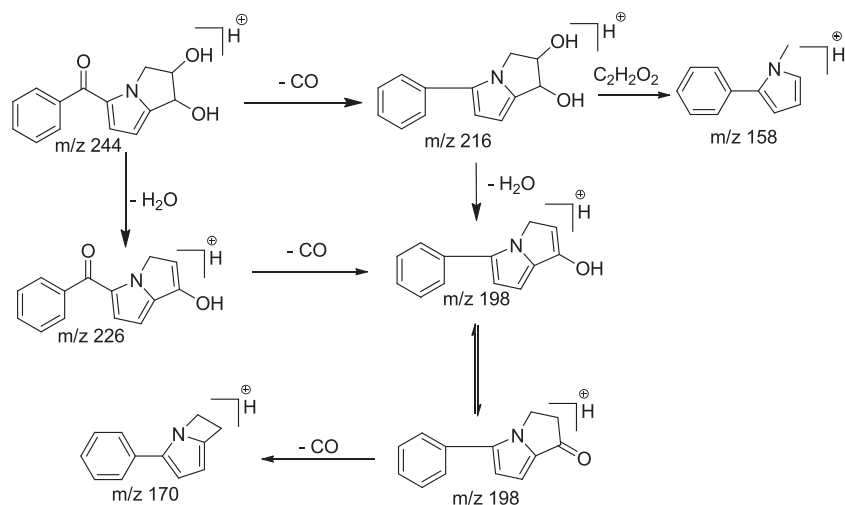
Oxidative degradation was performed in 6.0% H₂O₂ for 15 days. The drug degraded significantly after keeping the solution for 15 days in the dark room at an ambient temperature. A total of

three DPs, **K-5**, **K-6**, and **K-7**, were formed during oxidation (Fig. 1 (D), Scheme 5).

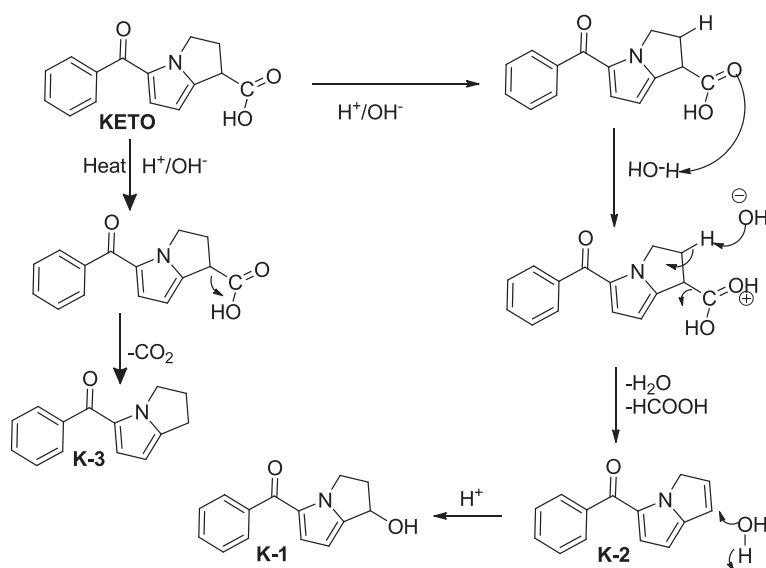
Photolytic degradation

On exposing the neutral solution of the drug at 1.2 million lux hours and 200 W h/m² for 15 days, three DPs (**K-1**, **K-6**, and **K-9**) were formed (Fig. 1(E)). In acidic drug solution, four DPs (**K-4**, **K-**

**Scheme 2.** Proposed fragmentation pathway of protonated ketorolac tromethamine (KETO) and its degradation products (**K-1**, **K-2**, **K-3**, **K-5**, **K-8**, and **K-9**).



Scheme 3. Proposed fragmentation pathway of degradant **K-4** (m/z 244).



Scheme 4. A probable mechanism of the formation of **K-1**, **K-2**, and **K-3** under hydrolytic conditions.

6, **K-8**, and **K-9**) were formed (Fig. 1(F)); whereas in alkaline drug solution, three DPs (**K-1**, **K-6**, and **K-9**) formed (Fig. 1(G)). Solid sample showed no formation of the DPs (Fig. 1(H)).

Thermal degradation

Thermal degradation sample showed formation of one DP, **K-3** (Fig. 1(I)).

LC/ESI/MS/MS study of KETO and its DPs

MS/MS of KETO

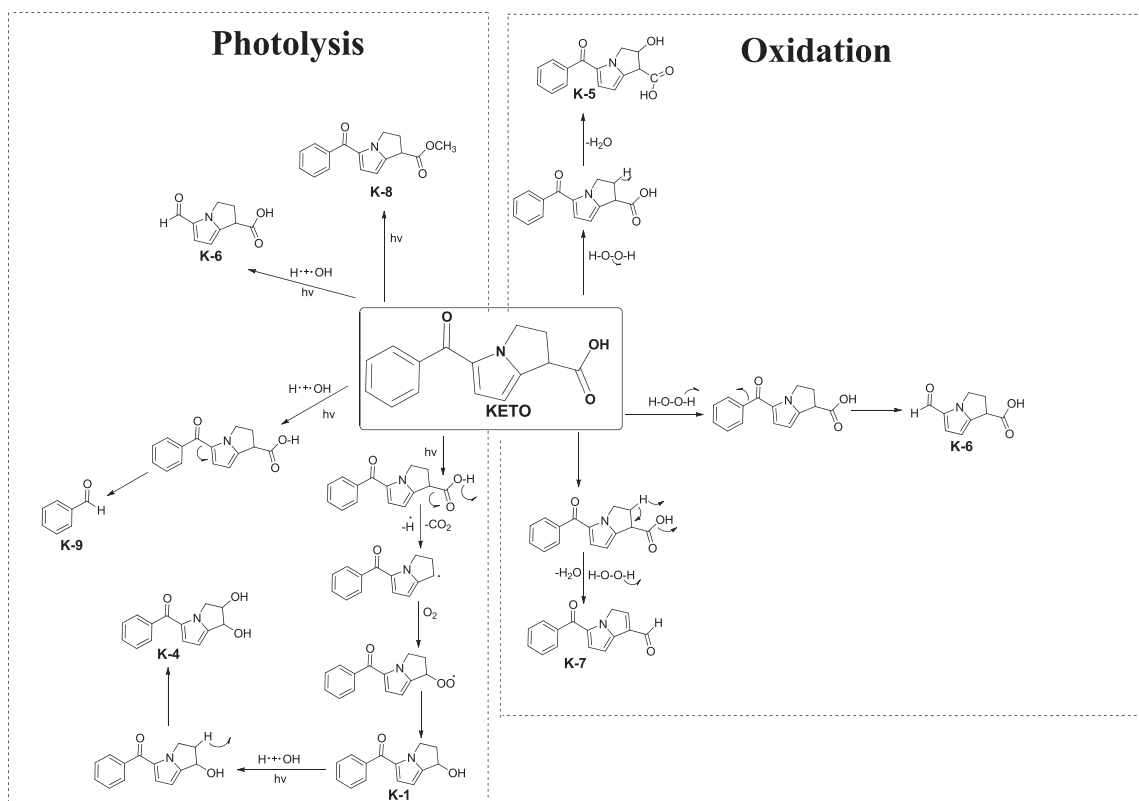
The MS/MS spectrum of protonated KETO ($R_t = 13.8$ min; $[m/z$ 256]) displays product ions at m/z 210 (loss of HCOOH), m/z 178 (loss C_6H_6 from m/z 256), m/z 132 (loss C_6H_6 from m/z 210), m/z 105 ($PhCO^+$), and m/z 77 ($C_6H_5^+$) (Fig. 2) (Scheme 2).^[23] It can be noted that m/z 105 is diagnostic for the presence of benzoyl group in KETO. The product ions at

m/z 178 and m/z 132 are characteristic for 2,3-dihydro-1H-pyrrolizine skeleton in KETO. The elemental compositions of all these ions have been confirmed by accurate mass measurements (Tables 2 and 3).

MS/MS of DPs

Online LC/ESI/MS/MS experiments were performed to characterize all the DPs (**K-1** to **K-9**) formed under various stress conditions. Most plausible structures have been proposed for all the DPs based on the m/z values of their $[M+H]^+$ ions and the MS/MS data in combination with elemental compositions derived from accurate mass measurements, as discussed in the succeeding texts.

The ESI/MS/MS spectrum of $[M+H]^+$ ion (m/z 228) of **K-1**, eluting at an R_t of 5.1 min (Fig. 2, Table 2), shows structure indicative fragment ions that are explained in Scheme 2. The molecular mass of **K-1** matches with impurity A, listed in British Pharmacopoeia.^[33] A mass difference of 27.9949 u (units)



Scheme 5. Probable mechanisms of formation of degradation products under oxidation and photolytic conditions.

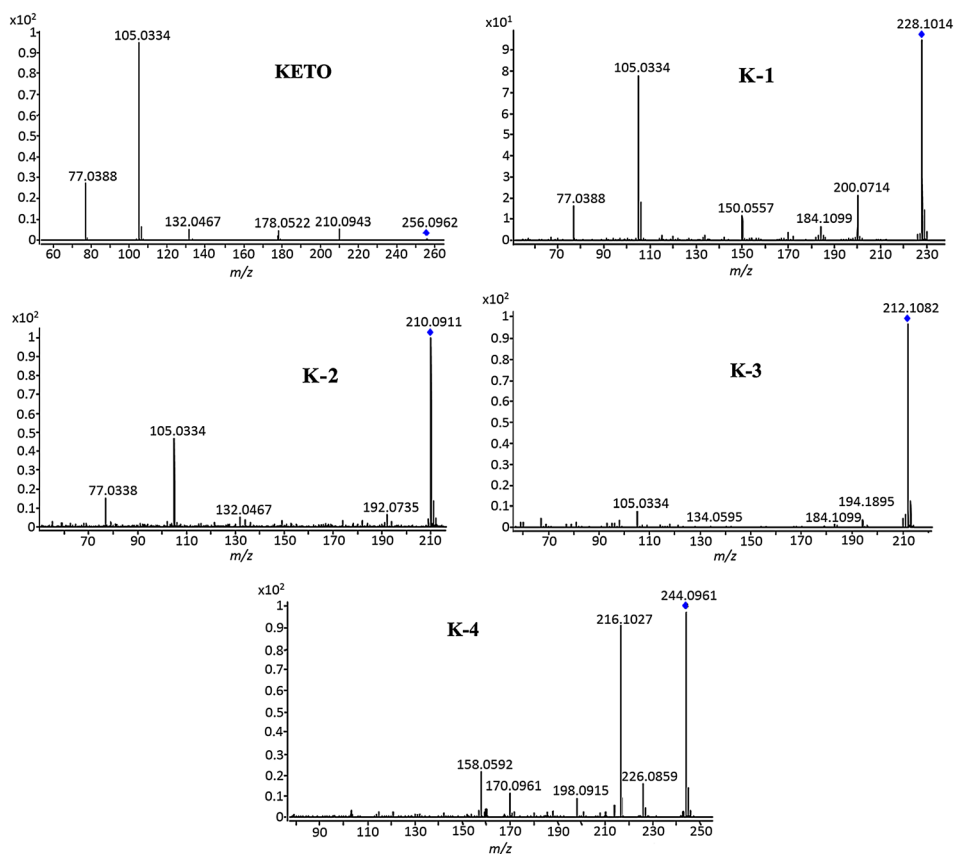


Figure 2. ESI/MS/MS spectrum of $[M + H]^+$ ions of ketorolac tromethamine (KETO) (m/z 206) at 20 eV, **K-1** (m/z 228) at 20 eV, **K-2** (m/z 210) at 15 eV, **K-3** (m/z 212) at 15 eV, and ESI/MS/MS spectrum of $[M + H]^+$ ions of **K-4** (m/z 244) at 20 eV.

Table 3. High resolution mass spectrometry (HRMS) data of product ions of protonated ketorolac tromethamine (KETO) and its degradation products

KETO and degradation product	Molecular formula [M + H] ⁺	Observed <i>m/z</i>	Calculated <i>m/z</i>	Error (ppm)
KETO	C ₁₅ H ₁₄ NO ₃ ⁺	256.0962	256.0959	-1.17
	C ₁₄ H ₁₂ NO ⁺	210.0943	210.0949	2.86
	C ₉ H ₈ NO ₃ ⁺	178.0522	178.0527	2.81
	C ₈ H ₇ NO ⁺	132.0467	132.0461	-4.54
	C ₇ H ₅ O ⁺	105.0334	105.0330	-3.81
	C ₆ H ₅ ⁺	77.0388	77.0391	3.89
K-1	C ₁₄ H ₁₄ NO ₂ ⁺	228.1014	228.1018	1.75
	C ₁₃ H ₁₄ NO ⁺	200.0714	200.0710	-2.00
	C ₁₃ H ₁₄ N ⁺	184.1099	184.1101	1.09
	C ₈ H ₈ NO ₂ ⁺	150.0557	150.0560	2.00
K-2	C ₁₄ H ₁₂ NO ⁺	210.0911	210.0914	1.43
	C ₁₄ H ₁₀ N ⁺	192.0735	192.0737	1.04
K-3	C ₁₄ H ₁₄ NO ⁺	212.1082	212.108	-0.94
	C ₁₄ H ₁₂ N ⁺	194.1895	194.1899	2.06
	C ₈ H ₈ NO ⁺	134.0595	134.0591	-2.98
K-4	C ₁₄ H ₁₄ NO ₃ ⁺	244.0961	244.0967	2.46
	C ₁₄ H ₁₂ NO ₂ ⁺	226.0859	226.0854	-2.21
	C ₁₃ H ₁₄ NO ₂ ⁺	216.1027	216.1023	-1.85
	C ₁₃ H ₁₂ NO ⁺	198.0915	198.0916	0.50
	C ₁₂ H ₁₂ N ⁺	170.0961	170.0965	2.35
K-5	C ₁₁ H ₁₂ N ⁺	158.0952	158.0958	3.80
	C ₁₅ H ₁₄ NO ₄ ⁺	272.0911	272.0913	0.74
	C ₁₅ H ₁₂ NO ₃ ⁺	254.0813	254.0817	1.57
	C ₉ H ₈ NO ₄ ⁺	194.0441	194.0443	1.03
K-8	C ₁₆ H ₁₅ NO ₃ ⁺	270.1131	270.1135	1.48
K-9	C ₇ H ₇ O ⁺	107.0495	107.0496	0.93

between **K-1** and KETO suggests that **K-1** is formed by the loss of carbonyl group and the presence of an abundant peak at *m/z* 105 in the MS/MS spectrum confirms that the CO comes from the carboxy group. The elemental compositions of [M + H]⁺ ion of KETO and its product ions have been confirmed by accurate mass measurements (Table 2). All these data are highly compatible with the proposed structure, (1-hydroxy-2,3-dihydro-1H-pyrrolizin-5-yl)(phenyl)methanone proposed for **K-1**. The formation of **K-1** in hydrolytic stress conditions can be explained by decarboxylation of KETO followed by an addition of —OH group from water (Scheme 4). A probable mechanism involving the decarboxylation, addition of oxygen, removal of singlet oxygen, and followed by addition of hydrogen radical for the formation of **K-1** under photolysis is illustrated in scheme 5.^[35]

A difference of 46 u between [M + H]⁺ ion of KETO and that of **K-2** (*m/z* 210) indicates that the latter is formed by loss of HCOOH from KETO, which has been supported by accurate mass measurements (Table 3). The ESI/MS/MS spectrum of [M + H]⁺ ion of **K-2** (*m/z* 210, Rt = 13.1 min) displays product ions that are also compatible with the structure, phenyl(3H-pyrrolizin-5-yl)methanone (Fig. 2, Table 2, Scheme 2). It can be noted that protonated **K-2** is also formed as a product ion of protonated KETO in its MS/MS spectrum. A probable mechanism for the formation of **K-2** under acidic hydrolytic condition is depicted in Scheme 4.

The [M + H]⁺ ion of **K-3** (Rt = 19.3 min) at *m/z* 212 (Fig 1, Table 2) and its elemental composition indicate that it is formed by loss of carbon dioxide (44 u) from KETO that is found to match with the

impurity I listed in British Pharmacopoeia.^[33] The product ions observed in the MS/MS spectrum (Fig. 2) are consistent with the structure (2,3-dihydro-1H-pyrrolizin-5-yl)(phenyl)methanone (Scheme 2). A probable mechanism for the formation of **K-3** is shown in Scheme 4. The elemental compositions of product ions have been confirmed by accurate mass measurements (Table 3).

Figure 2 shows the ESI/MS/MS spectrum of [M + H]⁺ ion (*m/z* 244) of **K-4** (Rt = 4.1 min) (Table 2). The spectrum displays high abundance [M + H]⁺ ion and its product ions at *m/z* 226 (loss of H₂O from *m/z* 244), *m/z* 216 (loss of CO from *m/z* 244), *m/z* 198 (loss of CO from *m/z* 226), *m/z* 170 (loss of CO from *m/z* 198), and *m/z* 158 (loss of C₂H₂O₂ from *m/z* 216) (Fig. 2). Proposed fragmentation pathway for **K-4** is given in Scheme 3, which has been supported by accurate mass measurements. On the basis of these information, **K-4** was identified as (1,2-dihydroxy-2,3-dihydro-1H-pyrrolizin-5-yl)(phenyl)methanone. A probable mechanism for the formation of **K-4** under photolytic condition is shown in Scheme 5.

The degradant **K-5** at *m/z* 272 [M + H]⁺ was eluted at 6.2 min, suggesting the addition of an oxygen to KETO (Fig. 3; Tables 2 and 3). The formation of a diagnostic ion at *m/z* 254 by the loss of H₂O confirms that **K-5** is a hydroxylated DP. The presence of an abundant ion at *m/z* 105 and absence of *m/z* 121 (hydroxy benzylation) rule out the hydroxylation in the aromatic ring. The elemental compositions of **K-5** and its product ions have been confirmed by accurate mass measurements (Tables 2 and 3). All these data are highly compatible with the proposed structure, 5-benzoyl-2-hydroxy-2,3-dihydro-1H-pyrrolizine-1-carboxylic acid (Scheme 2). A probable mechanism for the formation of **K-5** under oxidation may involve an addition of OH radical generated from hydrogen peroxide to KETO (Scheme 5).

The degradant **K-6** at *m/z* 178 was formed under oxidation, and a photolytic stress condition was eluted at 12.3 min (Table 2). The mass difference between the protonated drug (*m/z* 256) and **K-6** (*m/z* 178) is 78 u, which suggests the loss of benzene moiety from KETO (Scheme 5). The mass difference between protonated drug (*m/z* 256) and **K-7** (Rt = 15.5 min) is 18 u indicating that the latter is formed by loss of water molecule. The elemental compositions of [M + H]⁺ ions of **K-6** and **K-7** have been confirmed by accurate mass measurements (Tables 2 and 3). On the basis of these information, **K-6** and **K-7** were identified as 5-formyl-3H-pyrrolizine-1-carboxylic acid and 5-benzoyl-3H-pyrrolizine-1-carbaldehyde, respectively. Because of lower abundance of these ions, MS/MS experiments could not be performed.

The degradant **K-8** at *m/z* 270 ([M + H]⁺) was eluted at 7.2 min (Table 2). Molecular mass of **K-8** matched with the impurity H listed in British Pharmacopoeia.^[33] The increase of *m/z* value by 14 u indicates that **K-8** is a methylated DP (Scheme 1). Formation of the diagnostic product ion at *m/z* 210 from the protonated molecule by the loss of CH₃OH and CO confirms the methylation of COOH (Fig. 3, Scheme 2).^[35] The elemental compositions of **K-8** and its product ions have been confirmed by accurate mass measurements (Tables 2 and 3). A probable mechanism for the formation of **K-8** is shown in Scheme 5.

The ESI-MS/MS spectrum of [M + H]⁺ ion of **K-9** (*m/z* 107, Rt = 15.0 min) displays product ions that are compatible with the structure benzaldehyde (Fig. 3, Scheme 2, Table 2). The elemental compositions of **K-9** and its product ions have been confirmed by accurate mass measurements (Tables 2 and 3). A probable mechanism for the formation of **K-9** under photolytic condition is shown in Scheme 5.

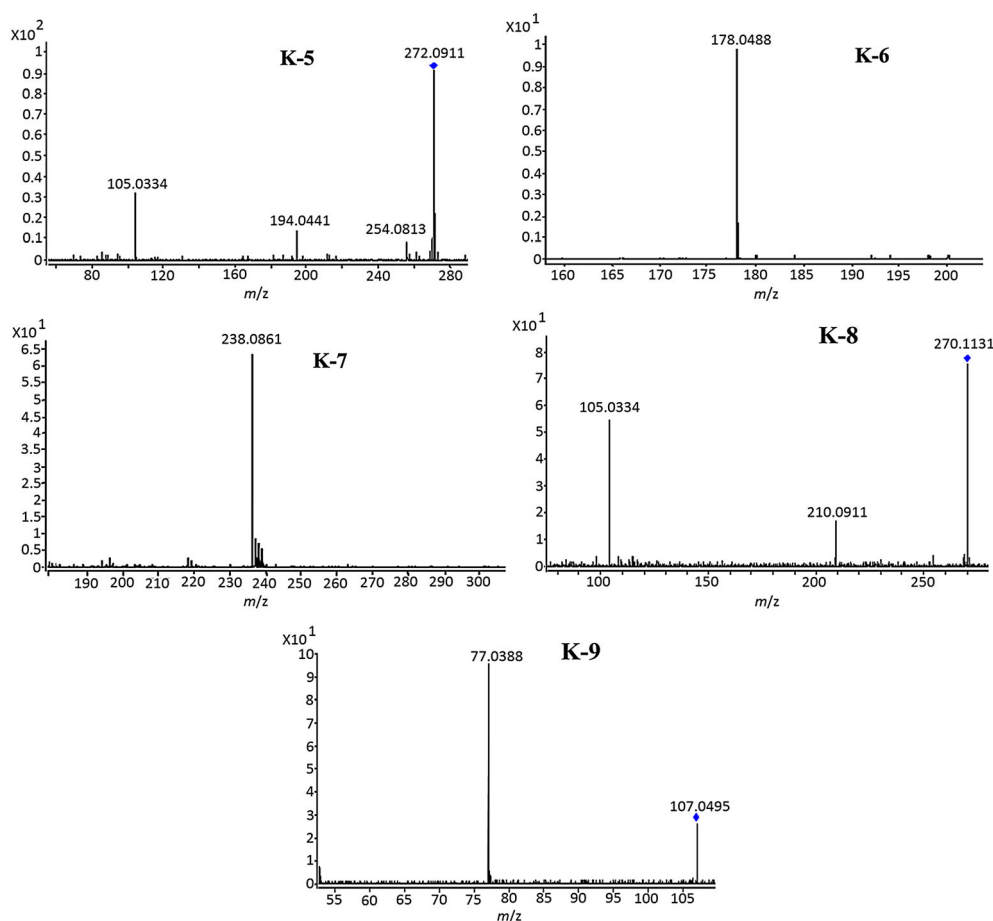


Figure 3. **K-5** (m/z 272) at 20 eV, **K-6** (m/z 178) at 15.0 eV, **K-7** (m/z 238) at 15 eV, ESI-MS/MS spectrum of $[M + H]^+$ ions of **K-8** (m/z 270) at 20 eV, and **K-9** (m/z 107) at 15 eV.

In silico toxicity prediction

The potential toxicity of KETO and its DPs were assessed by using TOPKAT and DEREK software.^[36] TOPKAT calculations were based on quantitative structure–toxicity relationship model using statistical methods such as linear regression of structural descriptors. Toxicity value generated through TOPKAT depends upon the LOG P, shape index, molecular weight, and symmetry of molecules. Probability values from 0.0 to 0.30 are considered low probabilities and are likely to produce a negative response in an experimental assay, whereas probability values greater than 0.70 are considered high and are likely to produce a positive response in an experimental assay. Probabilities greater than 0.30 but less than 0.70 are considered indeterminate. Tables 4.1 and 4.2 show the results of TOPKAT-predicted toxicity and carcinogenicity for KETO and its DPs. The toxicity of DPs were assessed and compared with KETO in different animal models. The probabilities of carcinogenicity of KETO in all the models are very less (<0.7) compared with DPs. All the DPs, except **K-1** and **K-4**, showed higher carcinogenicity potential in different models. For example, NTP Carcinogenicity Call (male mouse) (v3.2) model indicates higher probability of carcinogenicity for **K-2**, **K-3**, **K-7**, and **K-8** as compared with KETO. NTP Carcinogenicity Call (female mouse) (v3.2) showed higher probability of carcinogenicity for **K-6**, **K-7**, and **K-9** because of the presence of aldehyde group. Moreover, it is scientifically proven that aldehyde functional group may have high potential of genotoxicity and carcinogenicity.^[37]

Table 4.3 shows qualitative information on skin sensitization for KETO and its DPs, obtained using DEREK software. This rules-based software derived from the collective knowledge of toxicologists from academia, industry, and government. The toxicity predictions are the results of two processes. The program first checks whether any alerts in the knowledge base match toxicophores in the query structure. The reasoning engine then assesses the likelihood of a structure being toxic. There are nine levels of confidence: certain, probable, plausible, equivocal, doubted, improbable, impossible, open, and contradicted. DEREK can be integrated with Lhasa's Meteor software, which makes predictions of fate, thereby providing predictions of toxicity for both parent compounds and their degradants. The presence of α,β -unsaturated aldehyde structure alert in **K-7** may lead to its interaction with skin proteins via a Michael addition mechanism^[38] and therefore likely to cause skin sensitization.

Method validation

Specificity and linearity

Specificity of the method was determined by evaluating the peak purity of all DPs using photodiode array detector and also confirmed by subjecting all the stress samples to LC-MS analysis. The mass detector showed excellent purity of all DPs and the drug. Calibration curve was plotted by analysis of working standard solutions of KETO at six different concentrations in the

Table 4.1. Probability values of different toxicity models of the drug and its degradation products (K-1 to K-4) by TOPKAT analyses

Model	KETO	K-1	K-2	K-3	K-4
NTP Carcinogenicity Call (Male Rat) (v3.2)	0.002	0.000	0.000	0.002	0.000
NTP Carcinogenicity Call (Female Rat) (v3.2)	0.003	0.000	0.000	0.000	0.000
NTP Carcinogenicity Call (Male Mouse) (v3.2)	0.454	0.637	1.000	1.000	0.002
NTP Carcinogenicity Call (Female Mouse) (v3.2)	0.004	0.000	0.000	0.000	0.000
FDA Carcinogenicity Male Rat Non vsCarc (v3.1)	0.001	0.000	0.003	0.000	0.000
FDA Carcinogenicity Male Rat Single vsMult (v3.1)	0.000	0.000	0.000	0.000	0.000
FDA Carcinogenicity Female Rat Non vsCarc (v3.1)	0.000	0.000	0.000	0.000	0.002
FDA Carcinogenicity Female Rat Single vsMult (v3.1)	0.000	0.001	0.000	0.000	0.060
FDA Carcinogenicity Male Mouse Non vsCarc (v3.1)	0.004	0.001	0.000	0.000	0.000
FDA Carcinogenicity Male Mouse Single vsMult (v3.1)	0.024	0.000	0.221	0.000	0.000
FDA Carcinogenicity Female Mouse Non vsCarc (v3.1)	0.002	0.000	0.000	0.000	0.000
FDA Carcinogenicity Female Mouse Single vsMult (v3.1)	0.013	0.008	0.999	0.043	0.000
Weight of Evidence Carcinogenicity Call (v5.1)	0.002	0.051	1.000	0.383	0.033
Ames Mutagenicity (v3.1) ^a	0.000	0.000	0.000	0.000	0.999
Developmental Toxicity Potential (DTP) (v3.1)	0.000	0.000	0.000	0.001	0.003
Rat Oral LD50 (v3.1) (mg/kg) ^b	677.7	259.6	1700	24.2	1000
Rat Maximum Tolerated Dose – Feed/Water (v6.1) (mg/kg)	11.8	213.2	144.1	0.007	0.002
Rat Inhalational LC50 (v6.1) (g/m ³ /H) ^c	8.7	7.7	2.1	7.3	0.58
Chronic LOAEL (v3.1) (mg/kg) ^d	4.4	10.9	9.2	8.6	13.7
Skin Irritation (v6.1)	0.999	0.276	1.000	1.000	0.84
Skin Sensitization NEG v SENS (v6.1) ^e	1.000	0.002	1.000	1.000	0.000
Skin Sensitization MLD/MOD v SEV (v6.1)	1.000	0.139	1.000	0.002	1.000
Ocular Irritancy SEV/MOD vs MLD/NON (v5.1) ^f	0.993	0.000	0.000	0.000	0.000
Ocular Irritancy SEV vs MOD (v5.1)	0.000	0.082	0.000	0.000	0.000
Ocular Irritancy MLD vs NON (v5.1)	1.000	0.387	0.000	0.000	0.678
Aerobic Biodegradability (v6.1)	0.000	1.000	0.000	0.000	1.000
Daphnia EC50 (v3.1) (mg/l) ^g	0.313	728.1	0.046	0.138	550.1

NTP, National Toxicology Program; FDA, US Food and Drug Administration.
^aAmes mutagenicity test is a biological assay to measure the mutagenic potential of chemical compounds.
^bRat oral median lethal dose (LD50) in mg/kg.
^cRat inhalational median lethal concentration LC50 in g/m³/H.
^dChronic lowest observed adverse effect level (LOAEL).
^eFor a chemical, a computed probability less than 0.3 indicates a noncarcinogen (NEG) v sensitive (SENS)
^fSeverity specific submodels: NON (none), MLD (mild), MOD (moderate), and SEV (sever).
^gDaphnia median effective concentration (EC50) in mg/l.

range of 5.0–50.0 ng/ml. Each solution was injected and measured in triplicate ($n = 3$). Standard calibration curves were plotted by taking peak area on the y -axis and nominal concentrations of drug on the x -axis. Limits of detection and limits of quantification were calculated on the basis of signal-to-noise ratio that was determined by comparing measured signals from samples with known low concentrations of analyte with those of blank samples. For limits of detection and limits of quantification, signal-to-noise ratio is 3:1 and 10:1, respectively. Results obtained from the regression analysis of data are given in Table 5.

Accuracy

Accuracy was determined by applying the standard addition method to synthetic mixture of drug product placebo component to which known quantities of KETO had been spiked. Each solution was injected in triplicate analysis, and the percentage recovery was calculated. The percentage recovery range and %RSD values were found to be 99.0–101.0 and <2.0%, respectively (Table 6).

Precision

Precision of the developed method was measured in terms of intraday precision (repeatability) and interday precision (reproducibility). Method repeatability was determined from the results of five separate samples prepared at different concentrations. Each sample was injected in triplicate ($n = 3$), and peak areas obtained were used to calculate means and %RSD values. The method reproducibility was evaluated on four different days, by preparing and analyzing in triplicate five separate sample solutions at the same concentration of intraday solutions. Table 7 depicts %RSD for intraday and interday precision of method for KETO, and results (%RSD < 2.0%) show the method is precise in terms of intraday and interday precision (Table 9).

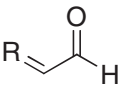
Robustness

Robustness measures reliability of an analytical method with respect to deliberate variations of the method parameters. Robustness of method was evaluated by changing the column temperature ($30 \text{ }^\circ\text{C} \pm 5.0 \text{ }^\circ\text{C}$), flow rate ($1.0 \pm 0.1 \text{ ml/min}$), and pH of the

Table 4.2. Probability values of different toxicity models of degradation products (K-5 to K-9) by TOPKAT analyses

Model	K-5	K-6	K-7	K-8	K-9
NTP Carcinogenicity Call (Male Rat) (v3.2)	0.008	0.000	0.000	0.092	0.030
NTP Carcinogenicity Call (Female Rat) (v3.2)	0.013	0.997	0.000	0.000	0.000
NTP Carcinogenicity Call (Male Mouse) (v3.2)	0.001	0.166	1.000	0.718	0.000
NTP Carcinogenicity Call (Female Mouse) (v3.2)	0.000	0.999	1.000	0.002	1.000
FDA Carcinogenicity Male Rat Non vsCarc (v3.1)	0.000	0.037	0.000	0.001	0.943
FDA Carcinogenicity Male Rat Single vsMult (v3.1)	0.000	0.000	0.000	0.000	0.626
FDA Carcinogenicity Female Rat Non vsCarc (v3.1)	0.992	0.000	0.000	0.000	0.997
FDA Carcinogenicity Female Rat Single vsMult (v3.1)	0.005	0.772	1.000	0.000	1.000
FDA Carcinogenicity Male Mouse Non vsCarc (v3.1)	0.002	0.010	0.001	0.000	0.393
FDA Carcinogenicity Male Mouse Single vsMult (v3.1)	0.000	0.000	0.001	0.187	0.783
FDA Carcinogenicity Female Mouse Non vsCarc (v3.1)	0.000	0.000	0.000	0.000	0.000
FDA Carcinogenicity Female Mouse Single vsMult (v3.1)	0.097	0.421	0.007	0.000	0.030
Weight of Evidence Carcinogenicity Call (v5.1)	0.005	0.002	0.000	0.006	0.238
Ames Mutagenicity (v3.1)	0.000	0.000	0.034	0.000	0.000
Developmental Toxicity Potential (DTP) (v3.1)	0.000	0.029	0.000	0.000	0.012
Rat Oral LD 50 (v3.1) (mg/kg)	3100	1200	683.7	544.9	1300
Rat Maximum Tolerated Dose – Feed/Water (v6.1) (mg/kg)	64	19.2	47.2	100	280.2
Rat Inhalational LC 50 (v6.1) (g/m ³ /H)	0.023	6.9	10.0	10	4.5
Chronic LOAEL (v3.1) (mg/kg)	3.1	20.7	30.2	8.0	170.0
Skin Irritation (v6.1)	1.000	1.000	1.000	1.000	0.014
Skin Sensitization NEG v SENS (v6.1)	1.000	1.000	1.000	1.000	0.961
Skin Sensitization MLD/MOD v SEV (v6.1)	1.000	0.999	1.000	1.000	0.993
Ocular Irritancy SEV/MOD vs MLD/NON (v5.1)	0.009	1.000	0.000	0.000	0.966
Ocular Irritancy SEV vs MOD (v5.1)	0.000	0.000	0.003	0.989	0.800
Ocular Irritancy MLD vs NON (v5.1)	1.000	1.000	1.000	0.044	0.061
Aerobic Biodegradability (v6.1)	0.075	1.000	1.000	0.000	1.000
Daphnia EC50 (v3.1) (mg/l)	445.1	2.7	0.209	15.9	12.9

Table 4.3. Qualitative toxicity prediction of the ketorolac tromethamine (KETO) and its degradation products (K-1 to K-9) by DEREK analyses

KETO and its degradation products	Skin sensitization
Structural alert	
Comments	R = any group (except OH) The skin sensitization of α,β -unsaturated aldehyde and precursors that interact with skin proteins via a Michael addition mechanism
KETO, K-1 to K-6, K-8, K-9	NA
K-7	√

mobile phase (3.2 ± 0.3) at three different concentrations (5, 30, and 50 ng/ml). Each sample was injected in triplicate ($n = 3$), and peak areas obtained were used to calculate means and % RSD values. The %RSD for the column temperature, flow rate, and the pH of the mobile phase was $< 1\%$. There were no significant changes in assay value of the drug that showed the robustness of the method.

Table 5. Parameters of linear regression equations for ketorolac tromethamine

Parameters	Value
Calibration range (ng/ml)	5.0–50.0
Correlation coefficient (r)	0.9999
Slope	12496
Intercept	–661.9
SD of slope	62.26
SD of intercept	1889.21
LOD (ng/ml)	0.52
LOQ (ng/ml)	1.48

SD, standard deviation; LOD, limits of detection; LOQ, limits of quantification.

Table 6. Accuracy study of ketorolac tromethamine using standard additions method ($n = 3$)

Spiked concentration (ng/ml)	Calculated spiked concentration (ng/ml) \pm SD; %RSD	Percent recovery
10.0	10.10 \pm 0.19; 1.91	101.0
30.0	29.81 \pm 0.49; 1.65	99.4
50.0	50.32 \pm 0.65; 1.29	100.6

Table 7. Intraday and interday precision study of ketorolac tromethamine ($n = 3$)

Concentration (ng/ml)	Intraday precision		Interday precision	
	Measured concentration (ng/ml) \pm SD; %RSD		Measured concentration (ng/ml) \pm SD; %RSD	
5.0	4.98 \pm 0.09; 1.87		4.99 \pm 0.096; 1.92	
10.0	10.03 \pm 0.10; 1.00		10.06 \pm 0.14; 1.43	
25.0	25.27 \pm 0.41; 1.62		25.27 \pm 0.473; 1.89	
40.0	39.68 \pm 0.66; 1.67		39.71 \pm 0.70; 1.76	
50.0	49.33 \pm 0.68; 1.39		49.33 \pm 0.845; 1.69	

Conclusion

A selective validated stability indicating LC/MS/MS method was developed to study the degradation behavior of KETO under hydrolysis (acid, base, and neutral), oxidation, photolysis, and thermal stress conditions and determined the inherent stability of the drug. The drug was found to degrade in all the stress conditions except when the solid was exposed to photolytic conditions. A total of nine unknown DPs were identified and characterized using online LC/ESI/MS/MS experiments combined with accurate mass measurements. The proposed structures of the DPs have been rationalized by appropriate mechanisms. This study may be useful in future investigation on characterization of process-related impurity. Further, *in silico* toxicities were predicted for all DPs using TOPKAT and DEREK softwares. NTP Carcinogenicity Call (female mouse) (v3.2) showed higher probability of carcinogenicity for **K-6**, **K-7**, and **K-9** because of the presence of aldehyde group. DEREK software shows structure alert for **K-7** that is likely to cause skin sensitization.

Acknowledgements

The authors thank Dr M. Lakshmi Kantam, Director, IICT, Hyderabad and Dr Ahmed Kamal, Project Director, NIPER, Hyderabad for facilities and their cooperation. P. K and D. N is thankful to the Ministry of Pharmaceuticals, New Delhi, for providing Junior Research Fellowship. B. R and R. B are thankful to CSIR (AARF) and DST, New Delhi, for awarding senior research fellowship.

References

- [1] K. M. Litvak, G. K. McEvoy, Ketorolac, an injectable nonnarcotic analgesic, *Clin. Pharm.* **1990**, *9*, 921.
- [2] R. W. Yee. Analgesic efficacy and safety of nonpreserved ketorolac tromethamine ophthalmic solution following radial keratotomy. *Am. J. Optha.* **1998**, *125*, 472.
- [3] D. J. Reinhart. Minimising the adverse effects of ketorolac. *Drug safe.* **2000**, *22*, 487.
- [4] FDA. Guideline for Submitting Documentation for the Stability of Human Drugs and Biologics. Food and Drug Administration: Rockville, MD, **1987**.
- [5] ICH guideline, Q1A (R2) Stability Testing of New Drug Substances and Products, *International Conference on Harmonisation, IFPMA, Geneva, Switzerland.*, **2000**.
- [6] S. Singh, T. Handa, M. Narayanam, A. Sahu, M. Junwal, R. P. Shah. A critical review on the use of modern sophisticated hyphenated tools in the characterization of impurities and degradation products. *J. Pharm. Biomed. Anal.* **2012**, *69*, 148.
- [7] B. Raju, M. Ramesh, R. Srinivas, R. S. Satyanarayana, Y. Venkateswarlu. Identification and characterization of stressed degradation products of prulifloxacin using LC-ESI-MS/Q-TOF, MSⁿ experiments: development of a validated specific stability-indicating LC-MS method. *J. Pharm. Biomed. Anal.* **2011**, *56*, 560.
- [8] R. M. Borkar, B. Raju, R. Srinivas, P. Patel, S. K. Shetty. Identification and characterization of stressed degradation products of metoprolol using LC/Q-TOF-ESI-MS/MS and MSⁿ experiments. *Biomed. Chromatogr.* **2012**, *26*, 720.
- [9] R. M. Borkar, B. Raju, P. S. Devrukhakar, T. Naresh, A. B. N. Nageswara Rao, R. Srinivas. Liquid chromatography/electrospray ionization tandem mass spectrometric study of milnacipran and its stressed degradation products. *Rapid Commun. Mass Spectrom.* **2013**, *27*, 369.
- [10] C. Purna chander, B. Raju, A. Sulthana, R. Srinivas. Liquid chromatography electrospray ionization tandem mass spectrometric (LC-ESI-MS/MS) study of carvedilol and its stress degradation products. *Anal. Meth* **2013**, *5*, 4330.
- [11] D. J. Jones, A. R. Bjorksten. Detection of ketorolac enantiomers in human plasma using enantioselective liquid chromatography. *J. Chromatogr. B Biomed. Sci. Appl.* **1994**, *661*, 165.
- [12] F. J. Flores-Murrieta, V. Granados-Soto, E. Hong. Determination of ketorolac in blood and plasma samples by high-performance liquid chromatography. *Boll. Chim. Farm.* **1994**, *133*, 588.
- [13] Z. Wang, R. M. Dsida, M. J. Avram. Determination of ketorolac in human plasma by reversed-phase high-performance liquid chromatography using solid-phase extraction and ultraviolet detection. *J. Chromatogr. B Biomed. Sci. Appl.* **2001**, *755*, 383.
- [14] S. Demircan, F. Sayin, N. E. Basci, N. Unlu, S. Kir. Determination of ketorolac tromethamine in human eye samples by HPLC with photo diode-array detection. *Chromatographia* **2007**, *66*, 135.
- [15] B. Raju, M. Ramesh, R. M. Borkar, R. Padiya, S. K. Banerjee, R. Srinivas. Development and validation of liquid chromatography-mass spectrometric method for simultaneous determination of moxifloxacin and ketorolac in rat plasma: application to pharmacokinetic study. *Biomed. Chromatogr.* **2012**, *26*, 1341.
- [16] I. Tsina, F. Chu, M. Kaloostian, M. Pettibone, A. Wu. HPLC method for the determination of ketorolac in human plasma. *J. Liq. Chromatogr. Relat Technol.* **1996**, *19*, 957.
- [17] I. Tsina, Y. L. Tam, A. Boyd, C. Rocha, I. Massey, T. Tarnowski. An indirect (derivatization) and a direct HPLC method for the determination of the enantiomers of ketorolac in plasma. *J. Pharm. Biomed. Anal.* **1996**, *15*, 403.
- [18] R. S. Chaudhary, S. S. Gangwal, K. C. Jindal, S. Khanna. Reversed-phase high-performance liquid chromatography of ketorolac and its application to bioequivalence studies in human serum. *J. Chromatogr. B Biomed. Sci. Appl.* **1993**, *614*, 180.
- [19] L. Franceschi, M. Furlanut. A simple and sensitive HPLC method to monitor serum and synovial fluid concentrations of ketorolac in reumatologic patients. *J. Bioanal Biomed.* **2010**, *2*, 121.
- [20] P. J. Hayball, J. G. Tamblyn, Y. Holden, J. Wrobel. Stereoselective analysis of ketorolac in human plasma by high-performance liquid chromatography. *Chirality* **1993**, *5*, 31.
- [21] K. R. Lorenzini, J. A. Desmeules, M. Besson, J.-L. Veuthey, P. Dayer, Y. Daali. Two-dimensional liquid chromatography-ion trap mass spectrometry for the simultaneous determination of ketorolac enantiomers and paracetamol in human plasma: application to a pharmacokinetic study. *J. Chromatogr. A* **2009**, *1216*, 3851.
- [22] M. A. Radwana, B. T. AlQuadeibb, N. M. Aloudaha, H. Y. Aboul Enein. Pharmacokinetics of ketorolac loaded to polyethylcyanoacrylate nanoparticles using UPLC MS/MS for its determination in rats. *Int. J. Pharm.* **2010**, *397*, 173.
- [23] B. Raju, M. Ramesh, R. M. Borkar, R. Padiya, S. K. Banerjee, R. Srinivas. Identification and structural characterization of *in vivo* metabolites of ketorolac using liquid chromatography electrospray ionization tandem mass spectrometry (LC/ESI-MS/MS). *J. Mass Spectrom.* **2012**, *47*, 919.
- [24] B. V. Kamath, K. Shivram, S. Vangani. Spectrophotometric determination of ketorolac tromethamine by charge transfer and ion-pair complexation. *Anal. Lett.* **1994**, *27*, 103.
- [25] P. V. Devarajan, S. P. Gore, S. V. Chavan. HPTLC determination of ketorolac tromethamine. *J. Pharm. Biomed. Anal.* **2000**, *22*, 679.
- [26] S. Orlandini, S. Furlanetto, S. Pinzauti, G. D'Orazio, S. Fanali. Analysis of ketorolac and its related impurities by capillary electrochromatography. *J. Chromatogr. A* **2004**, *1044*, 295.
- [27] J. C. Sturm, H. Canelo, L. J. Nunez-Vergara, J. A. Squella. Voltammetric study of ketorolac and its differential pulse polarographic determination in pharmaceuticals. *Talanta* **1997**, *44*, 931.

- [28] Z. Guorong, L. Wenhua, C. Shaofeng, S. Tianlin. Determination of ketorolac tromethamine by derivative adsorptive chronopotentiometry. *Chin. J. Anal. Chem.* **1998**, *10*, 022.
- [29] S. N. Razzaq, I. Mariam, I. U. Khan, M. Ashfaq. Development and validation of liquid chromatographic method for gatifloxacin and ketorolac tromethamine in combined dosage form. *J. Liq. Chromatogr. Relat Technol.* **2012**, *35*, 651.
- [30] S. N. Razzaq, I. U. Khan, M. Ashfaq, I. Mariam. Stability indicating HPLC method for simultaneous determination of moxifloxacin hydrochloride and ketorolac tromethamine in pharmaceutical formulations. *Quim. Nova.* **2012**, *35*, 1216.
- [31] K. Gandla, J. M. R. Kumar, D. Bikshapathi, R. Spandana. A validated RP-HPLC method for simultaneous estimation of febuxostat and ketorolac tromethamine in pharmaceutical formulations. *J. Drug Deliv Ther.* **2012**, *2*, 173.
- [32] M. Salaris, M. Nieddu, N. Rubattu, C. Testa, E. Luongo, M. G. Rimoli, G. Boatto. Acid and base degraded products of ketorolac. *J. Pharm. Biomed. Anal.* **2010**, *52*, 320.
- [33] British Pharmacopoeia, Vol. II, **2009**, pp. 1175.
- [34] ICH Q2(R1) International Conference on Harmonization (ICH) of Technical Requirements for Registration of Pharmaceuticals for Human Use, *Topic Q2 (R1): Validation of Analytical Procedures: Text and Methodology*, November **2005**.
- [35] H. H. Tonnesen, *The Photostability of Drugs and Drug Formulations*. Taylor & Francis Ltd: London, **2003**, 34.
- [36] N. F. Cariello, J. D. Wilson, B. H. Britt, D. J. Wedd, B. Burlinson, V. Gombar. Comparison of the computer programs DEREK and TOPKAT to predict bacterial mutagenicity. *Mutagenesis* **2002**, *17*, 321.
- [37] L. Muller, R. J. Mauthe, C. M. Riley, M. M. Andino, D. D. Antonis, C. Beels, J. DeGeorge, A. G. M. De Knaep, D. Ellison, J. A. Fagerland. A rationale for determining, testing, and controlling specific impurities in pharmaceuticals that possess potential for genotoxicity. *Regul. Toxicol. Pharmacol.* **2006**, *44*, 198.
- [38] G. F. Gerberick, C. A. Ryan, P. S. Kern, H. Schlatter, R. J. Dearman, I. Kimber, G. Y. Patlewicz, D. A. Basketter. Compilation of historical local lymph node data for evaluation of skin sensitization alternative methods. *Dermatitis.* **2005**, *16*, 157.